Published in final edited form as:
Am J Physiol Heart Circ Physiol. 2007 November ; 293(5): H3201–H3209. doi:10.1152/ajpheart.01363.2006.

CRYAB and HSPB2 deficiency alters cardiac metabolism and paradoxically confers protection against myocardial ischemia in aging mice

Ivor J. Benjamin[1], **Yiru Guo**[2], **Sathyanarayanan Srinivasan**[1], **Sihem Boudina**[3], **Ryan P. Taylor**[1], **Namakkal S. Rajasekaran**[1], **Roberta Gottlieb**[4], **Eric F. Wawrousek**[5], **E. Dale Abel**[3], and **Roberto Bolli**[2]

[1]Center for Cardiovascular Translational Biomedicine, University of Utah, School of Medicine, Salt Lake City, Utah [2]Institute of Molecular Cardiology, University of Louisville, Louisville, Kentucky [3]Program in Human Molecular Biology and Genetics, Division of Endocrinology and Metabolism, University of Utah, Salt Lake City, Utah [4]Department of Molecular and Experimental Medicine, The Scripps Research Institute, La Jolla, California [5]National Eye Institute, National Institutes of Health, Bethesda, Maryland

Abstract

The abundantly expressed small molecular weight proteins, CRYAB and HSPB2, have been implicated in cardioprotection ex vivo. However, the biological roles of CRYAB/HSPB2 coexpression for either ischemic preconditioning and/or protection in situ remain poorly defined. Wild-type (WT) and age-matched (~5–9 mo) CRYAB/HSPB2 double knockout (DKO) mice were subjected either to 30 min of coronary occlusion and 24 h of reperfusion in situ or preconditioned with a 4-min coronary occlusion/4-min reperfusion × 6, before similar ischemic challenge (ischemic preconditioning). Additionally, WT and DKO mice were subjected to 30 min of global ischemia in isolated hearts ex vivo. All experimental groups were assessed for area at risk and infarct size. Mitochondrial respiration was analyzed in isolated permeabilized cardiac skinned fibers. As a result, DKO mice modestly altered heat shock protein expression. Surprisingly, infarct size in situ was reduced by 35% in hearts of DKO compared with WT mice (38.8 ± 17.9 vs. 59.8 ± 10.6% area at risk, $P < 0.05$). In DKO mice, ischemic preconditioning was additive to its infarct-sparing phenotype. Similarly, infarct size after ischemia and reperfusion ex vivo was decreased and the production of superoxide and creatine kinase release was decreased in DKO compared with WT mice ($P < 0.05$). In permeabilized fibers, ADP-stimulated respiration rates were modestly reduced and calcium-dependent ATP synthesis was abrogated in DKO compared with WT mice. In conclusion, contrary to expectation, our findings demonstrate that CRYAB and HSPB2 deficiency induces profound adaptations that are related to *1*) a reduction in calcium-dependent metabolism/respiration, including ATP production, and *2*) decreased superoxide production during reperfusion. We discuss the implications of these disparate results in the context of phenotypic responses reported for CRYAB/HSPB2-deficient mice to different ischemic challenges.

Address for reprint requests and other correspondence: I. J. Benjamin, 30 N. 1900 E., Rm. 4A100, Salt Lake City, UT 84112 (ivor.benjamin@hsc.utah.edu)..

Keywords

small molecular weight heat shock protein; cardioprotection; aging; preconditioning; reperfusion injury

CRYAB and HSPB2 are two members of the multigene small heat shock proteins (sHSPs) family that are coexpressed in the mammalian heart, but the biological roles of which remain poorly defined. Among the ten sHSPs, CRYAB, the better known partner, has been implicated in stress-inducible translocation (8), antiapoptosis (19), remodeling of the cytoskeleton (27, 28), cardioprotection (23), and inheritable cardiomyopathy in humans (35). Earlier studies by Ray and coworkers (30) have demonstrated that CRYAB overexpression afforded powerful cardioprotection against ischemia and reperfusion in transgenic mice. On the other hand, little more is known about HSPB2 other than as a binding partner of dystrophin myotonic protein kinase, termed myotonic dystrophy protein kinase-binding protein (MKBP) in a two-hybrid screen (31). (The preferred name is HSPB2, instead of MKBP, suggested by an international nomenclature committee.)

Targeted deletions to define the biological functions of single genes comprise the majority of mouse knockout models, but disruptions of neighboring genes have been described occasionally. Both CRYAB and HSPB2, which are organized in head-to-head orientation in the genome and share a common bidirectional promoter (32), were deleted by this approach in mice (4). Double knockout CRYAB/HSPB2 (DKO) mice, for example, show histomorphological and ultrastructural abnormalities in aging skeletal muscle but are surprisingly devoid of cardiac histological and ultrastructural abnormalities (4). These intriguing findings suggest either that functional redundancy among the sHSPs family may compensate for CRYAB/HSPB2 deficiency or that more robust methodologies are needed to decipher subtle phenotypes and functional abnormalities in vivo or both.

To date, three independent groups have examined the functional requirements of CRYAB/HSPB2 deficiency in response to ischemic challenges using different experimental models (9, 17, 24). Consistent with the absence of morphological abnormalities, Morrison and coworkers (24) first demonstrated normal cardiac contractile function in DKO hearts at baseline but reduced contractile performance and increased apoptosis and necrosis compared with wild-type (WT) hearts using an ex vivo model of ischemia-reperfusion. In isolated papillary muscles, Golenhofen and colleagues (9) demonstrated that CRYAB/HSPB2 deficiency causes an earlier and higher peak ischemic contracture compared with control muscles. Furthermore, postischemic relaxation was delayed in DKO compared with controls, supporting the hypothesis CRYAB and HSPB2 play key roles in muscle maintenance and diastolic relaxation. Lastly, our laboratory has shown recently that DKO myocytes are more susceptible than control myocytes to simulated ischemic conditions (17), which support earlier findings reported by Morrison et al. (24). Although these studies provide complementary insights about their biological roles, in none could the investigators distinguish the requirements of one or both sHSPs.

Molecular properties of sHSP chaperones include stress-induced translocation onto intercalated disks, association with myofibrillar Z-lines structures, and interactions with the mitochondrial outer membrane. In a cultured cardiac-derived cell line, recent findings by Nakagawa and coworkers (26) indicate that HSPB2 is localized in cytoplasmic granules and selectively interacts with the outer mitochondrial membrane upon heat stress, suggesting potential effects on cardiac metabolism under stressful conditions. We hypothesize that the coexpression of CRYAB and HSPB2 serves unique biological roles in the mammalian heart,

especially during conditions associated with neurohormonal and other hemodynamic influences on prolonged postischemic adaptation in situ.

Here we report that DKO hearts undergoing pathophysiological challenge with ischemia-reperfusion are unexpectedly protected against myocardial ischemic damage in situ. Of interest, older (~5–9 mo) DKO mice used in these studies are devoid of cardiac abnormalities, supporting the potential relevance of these findings to understanding the mechanisms of ischemic vulnerability in the aging myocardium.

MATERIALS AND METHODS

Animals

These studies were approved by the Animal Care and Use Committees of the University of Texas Southwestern Medical Center (Dallas, TX), University of Louisville (Louisville, KY), and the University of Utah (Salt Lake City, UT), and with the *Guide for the Care and Use of Laboratory Animals* [Department of Health and Human Services, National Institutes of Health (NIH)].

DKO mice were generated using a targeting vector by Brady and coworkers (4) as described previously. DKO mice were bred in our colony into the 129S6/SvEvTac background; age and sex-matched WT controls were obtained from the Taconic Laboratories.

Morphological analysis

For hematoxylin and eosin staining, myocardial sections were deparaffinized and rehydrated to water, stained with Gill's hematoxylin (H3401, Vector) according to the manufacturer's instructions, and counterstained with eosin Y (E4382, Sigma). They were then dehydrated through graded alcohols to xylenes and mounted in a permanent mounting medium (27214, Ted Pella).

For Masson's trichrome staining, sections were deparaffinized and rehydrated to water and then transferred into Bouin's solution (HT10-1-32, Sigma) overnight at room temperature. After sections were rinsed in running tap water until they were colorless, nuclei were stained with Weigert's iron hematoxylin (HT10-79, Sigma), and the trichrome staining was completed using a kit (HT-15, Sigma) according to the manufacturer's instructions. The sections were then dehydrated through graded alcohols to xylenes and mounted in a permanent mounting medium. For electron-microscopic procedures, cryosections were processed for ultrastructural analysis of fixed myocardial cells and tissues by transmission electron microscopy using well-established methodologies (10). Immunohistofluorescence for CRYAB was performed as described recently by our laboratory (29).

In situ ischemic analysis

Experimental protocols were performed as described previously (13). For acute myocardial infarction, *group I* (WT) and *group II* (DKO) animals were subjected to 30 min of occlusion followed by 24 h reperfusion (Fig. 1*A*). For induction of early PC, *group III* (WT) and *group IV* (DKO) animals were subjected to a sequence of six cycles of 4-min coronary occlusion and 4-min reperfusion followed, 10 min later, by 30 min of coronary occlusion and 24 h of reperfusion (Fig. 1*A*). Thereafter, the mice were next injected intraperitoneally with heparin (1 U/g), anesthetized intravenously with pentobarbital sodium (35 mg/kg), and euthanized with an intravenous bolus of KCl. The heart was excised and perfused with Krebs-Henseleit solution through an aortic cannula (22- or 23-gauge needle) using a Langendorff apparatus. To assess infarcted from viable myocardium, the heart was then perfused with 1% solution of 2,3,5-triphenyltetrazolium chloride in phosphate buffer (pH 7.4, 37°C) at a pressure of 60

mmHg (~3 ml over 3 min). To delineate the occluded-reperfused coronary vascular bed, the coronary artery was then tied at the site of the previous occlusion and the aortic root was perfused with a 5% solution of phthalo blue dye (Heucotech, Fairless Hill, PA) in normal saline (2 ml over 3 min). In this procedure, the portion of the left ventricle (LV) supplied by the previously occluded coronary artery (region at risk) was identified by the absence of blue dye, whereas the rest of the LV was stained dark blue. The heart was frozen, after which all atrial and right ventricular tissues were excised. The LV was cut into 5–7 transverse slices, which were fixed in 10% neutral-buffered formaldehyde and, 24 h later, weighed and photographed (Nikon AF N6006). The transparencies were projected onto a paper screen at ×30 magnification, and the borders of the infarcted, ischemic reperfused and nonischemic regions were traced. The corresponding areas were measured by computerized videoplanimetry (Adobe Photoshop, version 4.0), and from these measurements the infarct size was calculated as a percentage of the region at risk.

Ex vivo ischemic analysis

WT and DKO mice were anesthetized with pentothal sodium (100 mg/kg), and the hearts were removed and placed in ice-cold Krebs-Ringer solution. The aortas were cannulated, and the hearts were perfused at a constant pressure of 60 mmHg with an oxygenated Krebs-Ringer buffer containing (in mM) 118 NaCl, 4.75 KCl, 1.18 KH_2PO_4, 1.18 $MgSO_4 \cdot 7H_2O$, 2.5 $CaCl_2$, 25 $NaHCO_3$, and 11 glucose. At the end of the reperfusion period, the hearts were stored at –20°C.

Measurement of infarct size was performed as previously described (16). Hearts were sliced into 1-mm sections, incubated in 1% triphenyltetrazolium (TTC) solution in PBS for 60 min at 37°C, and then fixed in 3.7% formaldehyde. Heart slices were scanned on a Hewlett-Packard Scanjet 5200C and analyzed with Adobe Photoshop 5.5. Images were subjected to equivalent manipulation of background, brightness, and contrast enhancement for improved clarity and brightness. Area at risk as well as infarct area of each slice was quantified, and the percent infarction was calculated as white pixels divided by the sum of red and white pixels.

Measurement of creatine kinase release

Coronary effluent was collected from the hearts at 5 min before global ischemia and for the first 5 min of reperfusion following ischemia. Creatine kinase (CK) enzyme activity was measured using the CK EC 2.7.3.2 UV-Test kit (Sigma) as per the manufacture's instructions.

Measurement of superoxide production

Superoxide production was measured via the conversion of dihydroethidium to ethidium as previously described (22). Hearts were sliced into 1-mm sections and incubated in 2 μM dihydroethidium in PBS for 20 min in the dark at 37°C. Sections were then placed on a microscope slide, and fluores-cent staining was viewed using an ultraviolet transilluminator (Fischer Scientific). Slices were photographed using a Kodak DC120 digital camera, and the image was analyzed using Adobe Photoshop 5.5. The percentage of superoxide production was quantified as the ratio of white fluorescent areas to the total heart area.

Western blot analysis

Heart homogenates were prepared in homogenization buffer containing 50 mM Tris (pH 7.5), 250 mM NaCl, 2 mM dithiothreitol, 1 mM phenylmethylsulfonyl fluoride, 10 μg/ml *p*-nitrophenyl phosphate leupeptin, 2 mM EDTA, 3 mM EGTA, 0.1 mM sodium orthovanadate, 1 mM, 10 μg/ml aprotinin, and 0.1% Triton X-100. Aliquots of the

supernatants (700 *g*) were prepared in Laemmli buffer, and 10 μl of the samples were loaded at 2 μg/μl protein concentrations for SDS-PAGE. The proteins were transferred to nitrocellulose membrane and were probed with antibodies against HSP25 (SPA801, Stressgen, British Columbia, Canada), HSP60 (SPA807, Stressgen), HSC70 (SPA812, Stressgen), and HSP90 (SPA835, Stressgen), and appropriate horseradish peroxidase-conjugated secondary antibodies (Vector, Burlingame, CA) were used. The proteins were detected using enhanced chemiluminescence reagents (Amersham Pharmacia), and images obtained on X-ray film were scanned and quantitated by densitometric analysis using the public domain NIH Image program (developed at the NIH and available at http://rsb.info.nih.gov/nih-image/). Graphs were generated after calculating the arbitrary units compared with WT.

Saponin-permeabilized fibers

Respiratory parameters of the total mitochondrial population were studied in situ in fresh saponin-permeabilized fibers as previously described (34). Briefly, small pieces (2–5 mg) of cardiac muscle were taken from the LV and permeabilized with 50 μg/ml saponin at 4°C in buffer A containing (in mM) 7.23 K_2EGTA, 2.77 K_2CaEGTA, 6.56 $MgCl_2$, 20 imidazole, 0.5 dithiothreitol, 53.3 K-methanS, 20 taurine, 5.3 Na_2ATP, 15 phosphocreatine, and 3 KH_2PO_4 (pH 7.1 adjusted at 25°C). The fibers were then washed twice for 10 min in buffer B containing (in mM) 7.23 K_2EGTA, 2.77 K_2CaEGTA, 1.38 $MgCl_2$, 20 imidazole, 0.5 dithiothreitol, 100 K-methanS, 20 taurine, and 3 KH_2PO_4 and 2 mg/ml BSA (pH 7.1 at 25°C).

Respiration and ATP measurements

The respiratory rates of saponin-permeabilized cardiac fibers were determined using an oxygen sensor probe in 2 ml buffer B at 25°C with continuous stirring. Studies were performed with three independent substrates: *1*) 5 mM glutamate and 2 mM malate and *2*) 0.02 mM palmitoyl-carnitine and 2 mM malate. The solubility of oxygen in buffer B is 215 nmol O_2/ml at 25°C. Oxygen consumption rates were expressed (in nmol) as O_2 (min/mg dry fiber wt). State 2 respiration (no ADP) was measured in a KCl solution containing the appropriate substrates. State 3 (ADP dependent) respiration was measured by adding ADP at a final concentration of 1 mM, which stimulates maximum activation of respiration. State 4 respiratory rate was measured by the addition of 1 μg/ml of oligomycin, an inhibitor of ATP synthase. As a measure of mitochondrial integrity, the respiratory control ratio, state 3 divided by state 4, was calculated. The data reported herein represent five independent mitochondrial preparations comprising two hearts each from a total of 10 WT and 10 DKO mice. ATP concentration was determined by a bioluminescence assay based on the luciferin/luciferase reaction using the ATP assay kit (ThermoLabsystems, Vantaa, Finland).

Statistical methods

For dichotomous background variables, the four groups subjected to ischemia-reperfusion and early PC in situ were compared using the Fisher-Freeman-Halton test, which is an extension of the Fisher exact test for larger than 2 × 2 cross tabulation tables. For continuous background variables, the four groups were compared using a one-way analysis of variance (ANOVA). All outcome variables were continuous measurements. To ensure comparability of the four mice groups, all outcomes were also compared using multivariable linear regression, controlling for both age and sex. The groups were similar in weight, so weight was omitted as a covariate. The model assumptions of normality and homogeneity of variance were checked using Shapiro-Wilks test for normality and Levene's test for homogeneity. In all of the comparisons, the normality assumption was satisfied. In the few comparisons, which violated the homogeneity of variance assumption, a robust variance estimate, also called the Huber-White sandwich estimator of variance, was incorporated into

the regression model to permit unequal group variances (14). The regression models were fit to two groups at a time, with all *P* values adjusted for six multiple comparisons using Finner's multiple comparison procedure (6). A two-way ANOVA was performed to analyze hemodynamic parameters. A single ANOVA was used to investigate respiration parameters. Mean value comparisons were performed by Student's *t*-test. Rate pressure product versus myocardial O_2 consumption ($M\dot{V}_{O_2}$) relationships were analyzed by linear regression analysis. A value of $P < 0.05$ was considered statistically significant (14).

RESULTS

Cardiac morphology

Brady and colleagues (4) have originally reported on the requirements of CRYAB/HSPB2 expression for skeletal muscle integrity and maintenance in mice, which was also corroborated by Morrison et al. (24). We have confirmed the absence of tissue abnormalities in the heart both at the level of light microscopy, after hematoxylin and eosin or trichrome staining, and ultrastructurally by electron microscopy (data not shown). Specifically, we demonstrate here the expected absence of histomorphological abnormalities and CRYAB immunostaining in 6-mo-old DKO compared with WT hearts by confocal microscopy (data not shown).

Animal characteristics

All experimental groups are in the isogenic 129S6 background, eliminating the contribution of genetic strain on potential differences in phenotype. Among the four experimental groups (I–IV), we found no significant differences in body weight, left ventricular mass (LV), or the region at risk (Table 1). We found no sex differences in this study (Table 1). Age-matched animals were subjected to either acute myocardial infarction (*groups I* and *II*) or early PC (*groups III* and *IV*), but statistical comparisons of infarct size were adjusted for sex and age using multivariable linear regression, with *P* values adjusted for six multiple comparisons using Finner's procedure (6) (Table 1). In addition, physiological parameters such as rectal temperature, heart rate, arterial blood pressure, and arterial blood gases were monitored and maintained throughout the experimental protocol.

In situ ischemic tolerance

To investigate the role of CRYAB/HSPB2 coexpression in vivo, WT (*group I*) and DKO (*group II*) mice, without prior PC or sham manipulation (data not shown), were subjected to 30 min of coronary occlusion followed by 24 h of reperfusion in vivo. In WT mice, the infarct size was 58.8 ± 3.4% of the region of risk compared with 36. ± 7.9% in the DKO mice ($P < 0.05$) (Fig. 1), indicating that CRYAB-HSPB2 deficiency has an unexpected salutary effect on ischemic vulnerability in situ.

Since the magnitude of CRYAB/HSPB2 deficiency on ischemic protection mimics a PC effect, we next examined whether these sHSPs play a direct role in the early phase of ischemic PC. As described previously (12), we performed six 4-min occlusion/4-min reperfusion cycles, followed 10 min later by 30 min of coronary occlusion and 24 h of reperfusion in situ. Acid-base balance, adequate oxygenation, and maneuvers to prevent either hypothermia or hypotension were monitored and were found to be similar in our experimental groups throughout the procedure (data not shown) (12). In WT mice (*group III*) with PC, the infarct size of the heart was 31.7 ± 5.5% of the risk region (Fig. 1, *B* and *C*), indicating an ischemic PC effect (*group I* vs. *group III*, $P < 0.05$). In DKO mice with similar prior PC manipulation, the infarct size was 18.7 ± 3.0% of the risk region (Fig. 1), indicating a 50% reduction compared with DKO mice without PC and, therefore, consistent with an early ischemic PC effect.

Ex vivo ischemic tolerance

Like the studies in situ, the isolated perfused hearts of DKO mice sustained significantly smaller infarcts after ischemia and reperfusion than the WT controls (Fig. 2*A*). This was supported by the finding that CK release was diminished in the DKO mice (Fig. 2*B*). We found that superoxide production in the isolated perfused heart of DKO mice following global ischemia and reperfusion was substantially attenuated ($P < 0.05$) compared with WT mice (Fig. 2*C*).

HSP protein expression

To investigate whether CRYAB/HSPB2 deficiency altered the basal HSP expression, representative members of the major HSP classes were assessed by Western blot analysis in age-matched WT and DKO animals (Fig. 3). In both WT and DKO hearts, several HSP isoforms were unchanged (e.g., HSP90 and HSP70), whereas others, such as HSP25, were decreased in the cytosolic soluble fraction and increased in the cytoskeletal/nuclear pellet from DKO animals, suggesting interdependent relationships among sHSPs in vivo.

Skinned fiber respiration and ATP synthesis

To determine whether mitochondrial function might be altered by CRYAB/HSPB2 deficiency, we assessed mitochondrial respiration rates using skinned fibers from the myocardium. Mitochondrial respiration was determined in skinned fibers using either 5 mM glutamate/2 mM malate or 0.02 mM palmitoyl carnitine/2 mM malate as substrates, respectively (Fig. 4). In cardiac skinned fibers of DKO mice, state 2 and state 3 (ADP stimulated) respiration, but not state 4, was reduced by 22% and 19%, respectively, compared with WT hearts using glutamate/malate as substrate ($P < 0.005$ and $P < 0.01$, respectively). In contrast, with the use of palmitoyl-carnitine/malate as substrate, state 3 and state 4, but not state 2, respiration was reduced by 26% and 32%, respectively, in DKO compared with WT mice ($P < 0.05$ and 0.01, respectively), indicating a profound effect on mitochondrial respiration by DKO deficiency. In skinned fibers of DKO mice, the marked attenuation of state 4 respiration was similarly associated with a significant reduction of ATP production by 62% compared with that in WT hearts (Fig. 5), suggesting profound alterations in the coupling of respiration to ATP production.

DISCUSSION

In the present study, we report that DKO hearts of CRYAB/HSPB2-deficient mice are remarkably resistant to ischemiareperfusion in situ. Our novel findings were confirmed using an ex vivo experimental preparation in which myocardial injury and superoxide production were significantly decreased in DKO hearts compared with WT animals after ischemia-reperfusion. Because DKO hearts still responded to classical early PC, our data suggest that sHSPs, such as CRYAB and HSPB2, are not required for this cardioprotective phenotype. CRYAB/HSPB2 deficiency dramatically alters the translocation of HSP25 between the soluble and insoluble fractions (Fig. 3*A*), suggesting the need for future studies to explore potential posttranslational mechanisms in subcellular localization of sHSPs in vivo. Significant differences in mitochondrial respiration and ATP production were present in DKO hearts. These data for the first time suggest that CRYAB and HSPB2 exert novel roles in cardiac metabolic reserve and mitochondrial function in the postischemic heart in situ.

Ex vivo animal models have provided useful information on cardiac contractile performance but without the confounding influences of neurohormonal, hemodynamic, and other compensatory/adaptive factors (11). The reliability of the experimental preparation decreases as the duration of ischemia increases with the greatest confidence associated with

early to midreperfusion times; furthermore, this discordance between myocyte viability and functional parameters increases with longer (~180 min) reperfusion periods (30). Our findings contrast sharply with the results on postischemic functional recovery ex vivo but with several noteworthy differences. To date, three independent groups, including our using different experimental preparations of the same DKO model, have addressed specific questions related to ischemic challenges but have uncovered conflicting findings, creating unanswered questions with important implications for the field (9, 17, 24). In Morrison's experimental preparation, DKO hearts were subjected to 30 min equilibration, 25 min no-flow (global) ischemia, and 90 min reperfusion. Decreased contractile recovery in postischemic DKO hearts ex vivo correlated with increased necrosis and apoptosis, which were assessed by myoglobin release and DNA fragmentation [i.e., transferase-mediated dUTP nick-end labeling (TUNEL) assay], respectively (24).

In isolated papillary muscles, Golenhofen and colleagues (9) demonstrated an earlier and higher peak ischemic contracture in DKO compared with control muscles. Furthermore, postischemic relaxation was delayed in DKO and not with the controls, supporting the hypothesis that CRYAB and HSPB2 play key roles in muscle maintenance and diastolic relaxation. Our laboratory has reported recently that DKO myocytes are more susceptible than control myocytes to simulated ischemic conditions (17), which support earlier findings reported by Morrison et al. (24). In the present study, DKO hearts were subjected to a 15-min stabilization period followed by 30 min global of ischemia and 120 min of reperfusion ex vivo. Postischemic contractile function was not assessed directly, but both infarct size by TTC staining and enzyme leak (i.e., CK release) were significantly decreased in DKO compared with controls hearts. Since both groups used the same genetic model (4), we suggest that the differences in ischemic duration (25 vs. 30 min) and end points analyzed may account for the discordance between postischemic contractility and myocardial injury.

The most significant finding of the present study was that our results on the infarct-sparing effects of CRYAB/HSPB2 deficiency ex vivo were independently confirmed using a complementary approach in the postischemic heart in situ, which incorporates both neurohormonal and other compensatory factors. Both apoptosis and necrosis are the major mechanisms for myocardial injury (18), but TTC staining permits quantitative determination of widely accepted qualitative end points; red staining indicates viable tissue, and white shows infracted tissue. Smaller infarct size and increased TTC staining in both ex vivo and in situ models, therefore, indicates that CRYAB/HSPB2 deficiency contributes to increased myocardial viability and, correspondingly, decreased necrosis and/or apoptosis. When analyzed by a multivariate linear regression model, which controls for age and sex, these outcome variables between DKO and controls remained significant. Since transgenic CRYAB overexpression in mice has been shown to reduce both myocardial necrosis and apoptosis (30), these findings suggest that either that CRYAB and HSPB2 exert antagonistic roles in cell survival/death pathways or that CRYAB/HSPB2 deficiency per se has favorable effects on myocardial salvage after ischemia-reperfusion in situ.

Ischemic PC is the most powerful maneuver for myocardial salvaging in mammals including humans (25, 38, 39). Because 7 out of 10 sHSPs are predominantly expressed in the heart and skeletal muscle (33) and because CRYAB expression accounts for 1–3% soluble heart homogenates, we had previously hypothesized that sHSPs such as CRYAB might mediate ischemic PC through its cytoskeletal protective functions (3). Remarkably, the infarct-sparing effects of early PC were additive to the conditional state in DKO hearts, strongly suggesting for the first time that neither CRYAB nor HSPB2 is required for classical PC in vivo. These findings are consistent with early studies by Armstrong and coworkers (1) who convincingly showed that neither phosphorylated nor translocated CRYAB correlated with classical PC in isolated rabbit cardiomyocytes. Taken together, we agree with Golenhofen

and colleagues (9) that the CRYAB/HSPB2 mutant model remains a robust experimental tool for studies of the in vivo functions of sHSPs.

What other molecular mechanism(s) in cardiac physiology and ischemic cardioprotection might be uncovered from studies of CRYAB/HSPB2 deficiency in mice? Decreased ischemic contracture in isolated DKO hearts ex vivo (24) and the earlier increased tension in isolated papillary muscles during ischemia (9) are consistent with important roles and requirements of CRYAB expression per se for cytoskeletal remodeling and muscle maintenance. Among possible molecular targets and client proteins, CRYAB has been shown to bind macromolecular titin, which spans the half sarcomere from the M-line to the Z-disk, thereby affording protection from ischemia-induced protein aggregation and misfolding (5).

The present study also suggests that CRYAB and/or HSPB2 deficiency may have hitherto unrecognized effects on cardiac metabolism and functional adaptation in vivo. Our studies in permeabilized fibers of cardiac tissues reveal a modest reduction in ADP-stimulated respiration rates, but a more dramatic reduction in ATP synthesis in DKO compared with control hearts (Fig. 5). It is unlikely that a defect in electron-transport chain flux could account for the disproportionate reduction in ATP generation. If so, a proportionate reduction in mitochondrial respiration rates and ATP generation would then be expected. Thus the possibility exists that the observed defect may reflect either a primary reduction in ATP generation by ATP synthase or decreased export of ATP from the mitochondria. Since calcium is an important physiological stimulus for ATP synthesis (2, 15, 20, 21), then the abrogation of calcium signaling in DKO is predicted to decrease mitochondrial F1F0 ATP synthase. In addition, potential mechanisms for decreased ATP synthesis may include a reduction in the mitochondrial membrane potential on the basis of mitochondrial uncoupling or reduced catalytic efficiency of ATP synthase (7).

Of interest, cardiac performance was not reduced in proportion to $M\dot{V}_{O_2}$ in isolated DKO hearts perfused with glucose and palmitate as substrates, indicating increased myocardial contractile efficiency (data not shown). A possible explanation for this is a switch in myocardial substrate preference toward more metabolically efficient substrates. If this was indeed the case, we would predict that, compared with WT mice, DKO mice would have increased rates of glucose oxidation relative to fatty acid oxidation.

Limitations and future directions

We recognize that infarct size and cardiac function might be differentially affected by the DKO, especially in the intact heart where influences from neurohormonal, compensatory, and other adaptive factors outside the heart are integrated. Cardiac functional assessments, such as positron emission tomography or cardiac catheterization miniaturized for mouse work, will be needed to explore such mechanisms after ischemia-reperfusion in situ. Such maneuvers are demanding, technically challenging, and require expensive equipment. Nonetheless, using shorter period of no-flow ischemia (i.e., 15 min) and similar ex vivo protocols, we have uncovered important differences in myocardial performance and cardiac energetics between DKO and WT controls using NMR spectroscopy (unpublished results).

Based on the present findings, there is credible evidence to search molecular targets of CRYAB/HSPB2 interactions implicated in calcium homeostasis and/or mitochondrial respiration or both. In isolated cardiac myocytes subjected to metabolic inhibition, CRYAB/HSPB2 deficiency increases mitochondrial permeability transition (MPT) using the fluorescent dye tetramethylrhodamine methyl ester (17). However, mitochondria swelling as a marker of MPT opening was indistinguishable between isolated WT and DKO hearts (data not shown). We envision that CRYAB and HSPB2 might serve specific roles as docking

partners for mitochondrial preproteins at the outer membrane and/or directly with the translocase of the outer mitochondrial membrane complex (reviewed in Refs. 36 and 37). Although disparate phenotypes may preclude the definitive assignment to a single gene product, the effects of CRYAB/HSPB2 deficiency in mice provide unique opportunities to understand potential combinatorial roles of CRYAB/HSPB2 in vivo. Future studies with CRYAB or HSPB2 gene replacement or single knockout models could clarify these hypotheses and determine whether the present phenotypes of CRYAB/HSPB2-deficient mice are secondary rather than primary adaptive mechanisms.

In summary, we report here surprising findings that CRYAB/HSPB2 deficiency decreases rather than increases ischemic damage in the metabolically active heart during pathophysiological adaptation to ischemia-reperfusion in situ. These findings directly implicate novel roles for CRYAB and HSPB2 coexpression in mitochondrial metabolism, a key mediator of both oxidative and nitrosative stresses. The existence of a critical lesion at the level of the $M\dot{V}_{O_2}$ suggests that CRYAB/HSPB2 interaction with signaling pathways may trigger reactive nitrogen or oxygen species of mitochondrial origin during ischemia-reperfusion. Because mutations in CRYAB have been linked to human diseases including myopathy and cardiomyopathy (35) and because HSPB2 by binding to the myotonic dystrophy protein kinase has been indirectly linked to myotonic dystrophy (31), further studies of CRYAB and HSPB2 have potential medical relevance to molecular pathogenesis and disease prevention.

Acknowledgments

We appreciate the helpful suggestions and comments from members of the Benjamin Laboratory. Kelley Murphy and Krista Boeger provided superb editorial assistance during preparation of this manuscript. We are indebted to Greg Stoddard for expert assistance with statistical analyses used in this study.

GRANTS

This work was supported by National Heart, Lung, and Blood Institute Grant 5RO1-HL-63834 (to I. J. Benjamin).

REFERENCES

1. Armstrong SC, Shivell CL, Ganote CE. Differential translocation or phosphorylation of alpha B crystallin cannot be detected in ischemically preconditioned rabbit cardiomyocytes. J Mol Cell Cardiol. 2000; 32:1301–1314. [PubMed: 10860771]
2. Balaban RS. Cardiac energy metabolism homeostasis: role of cytosolic calcium. J Mol Cell Cardiol. 2002; 34:1259–1271. [PubMed: 12392982]
3. Benjamin IJ, McMillan DR. Stress (heat shock) proteins: molecular chaperones in cardiovascular biology and disease. Circ Res. 1998; 83:117–132. [PubMed: 9686751]
4. Brady JP, Garland DL, Green DE, Tamm ER, Giblin FJ, Wawrousek EF. AlphaB-crystallin in lens development and muscle integrity: a gene knockout approach. Invest Ophthalmol Vis Sci. 2001; 42:2924–2934. [PubMed: 11687538]
5. Bullard B, Ferguson C, Minajeva A, Leake MC, Gautel M, Labeit D, Ding L, Labeit S, Horwitz J, Leonard KR, Linke WA. Association of the chaperone alphaB-crystallin with titin in heart muscle. J Biol Chem. 2004; 279:7917–7924. [PubMed: 14676215]
6. Finner H. On a monotonicity problem with in step-down multiple test procedures. J Amer Stat Assoc. 1993; 88:920–923.
7. Fleury C, Sanchis D. The mitochondrial uncoupling protein-2: current status. Int J Biochem Cell Biol. 1999; 31:1261–1278. [PubMed: 10605819]
8. Golenhofen N, Ness W, Koob R, Htun P, Schaper W, Drenckhahn D. Ischemia-induced phosphorylation and translocation of stress protein αB-crystallin to Z lines of myocardium. Am J Physiol Heart Circ Physiol. 1998; 274:H1457–H1464.

9. Golenhofen N, Redel A, Wawrousek EF, Drenckhahn D. Ischemia-induced increase of stiffness of alphaB-crystallin/HSPB2-deficient myocardium. Pflügers Arch. 2006; 451:518–525. [PubMed: 16217658]
10. Griffiths, G. Fine Structure Immunohistochemistry. Springer-Verlag; New York: 1993.
11. Grupp IL, Subramaniam A, Hewett TE, Robbins J, Grupp G. Comparison of normal, hypodynamic, and hyperdynamic mouse hearts using isolated work-performing heart preparations. Am J Physiol Heart Circ Physiol. 1993; 265:H1401–H1410.
12. Guo Y, Jones WK, Xuan YT, Tang XL, Bao W, Wu WJ, Han H, Laubach VE, Ping P, Yang Z, Qiu Y, Bolli R. The late phase of ischemic preconditioning is abrogated by targeted disruption of the inducible NO synthase gene. Proc Natl Acad Sci USA. 1999; 96:11507–11512. [PubMed: 10500207]
13. Guo Y, Wu WJ, Qiu Y, Tang XL, Yang Z, Bolli R. Demonstration of an early and a late phase of ischemic preconditioning in mice. Am J Physiol Heart Circ Physiol. 1998; 275:H1375–H1387.
14. Hamilton, L. Statistics with Stata: Updated for Version 9. Thomson Brooks/Cole; Belmont, CA: 2006.
15. Hansford RG, Zorov D. Role of mitochondrial calcium transport in the control of substrate oxidation. Mol Cell Biochem. 1998; 184:359–369. [PubMed: 9746330]
16. He H, Chen M, Scheffler NK, Gibson BW, Spremulli LL, Gottlieb RA. Phosphorylation of mitochondrial elongation factor Tu in ischemic myocardium: basis for chloramphenicol-mediated cardioprotection. Circ Res. 2001; 89:461–467. [PubMed: 11532908]
17. Kadono T, Zhang XQ, Srinivasan S, Ishida H, Barry WH, Benjamin IJ. CRYAB and HSPB2 deficiency increases myocyte mitochondrial permeability transition and mitochondrial calcium uptake. J Mol Cell Cardiol. 2006; 40:783–789. [PubMed: 16678848]
18. Kajstura J, Cheng W, Reiss K, Clark WA, Sonnenblick EH, Krajewski S, Reed JC, Olivetti G, Anversa P. Apoptotic and necrotic myocyte cell deaths are independent contributing variables of infarct size in rats. Lab Invest. 1996; 74:86–107. [PubMed: 8569201]
19. Kamradt T, Goggel R, Erb KJ. Induction, exacerbation and inhibition of allergic and autoimmune diseases by infection. Trends Immunol. 2005; 26:260–267. [PubMed: 15866239]
20. McCormack JG, Denton RM. Mitochondrial Ca^{2+} transport and the role of intramitochondrial Ca^{2+} in the regulation of energy metabolism. Dev Neurosci. 1993; 15:165–173. [PubMed: 7805568]
21. McCormack JG, Denton RM. The role of intramitochondrial Ca^{2+} in the regulation of oxidative phosphorylation in mammalian tissues. Biochem Soc Trans. 1993; 21:793–799. [PubMed: 8224512]
22. Miller FJ Jr, Gutterman DD, Rios CD, Heistad DD, Davidson BL. Superoxide production in vascular smooth muscle contributes to oxidative stress and impaired relaxation in atherosclerosis. Circ Res. 1998; 82:1298–1305. [PubMed: 9648726]
23. Morrison LE, Hoover HE, Thuerauf DJ, Glembotski CC. Mimicking phosphorylation of alphaB-crystallin on serine-59 is necessary and sufficient to provide maximal protection of cardiac myocytes from apoptosis. Circ Res. 2003; 92:203–211. [PubMed: 12574148]
24. Morrison LE, Whittaker RJ, Klepper RE, Wawrousek EF, Glembotski CC. Roles for αB-crystallin and HSPB2 in protecting the myocardium from ischemia-reperfusion-induced damage in a KO mouse model. Am J Physiol Heart Circ Physiol. 2004; 286:H847–H855. [PubMed: 14592939]
25. Murry CE, Jennings RB, Reimer KA. Preconditioning with ischemia: a delay of lethal cell injury in ischemic myocardium. Circulation. 1986; 74:1124–1136. [PubMed: 3769170]
26. Nakagawa M, Tsujimoto N, Nakagawa H, Iwaki T, Fukumaki Y, Iwaki A. Association of HSPB2, a member of the small heat shock protein family, with mitochondria. Exp Cell Res. 2001; 271:161–168. [PubMed: 11697892]
27. Paulin D, Huet A, Khanamyrian L, Xue Z. Desminopathies in muscle disease. J Pathol. 2004; 204:418–427. [PubMed: 15495235]
28. Paulin D, Li Z. Desmin: a major intermediate filament protein essential for the structural integrity and function of muscle. Exp Cell Res. 2004; 301:1–7. [PubMed: 15501438]
29. Rajasekaran NS, Connell P, Christians ES, Yan LJ, Taylor RP, Orosz A, Zhang XA, Stevenson TJ, Peshock RM, Leopold JA, Barry WH, Loscalzo J, Odelberg SJ, Benjamin IJ. Human alphaB-

crystallin causes oxido-reductive stress and protein aggregation cardiomyopathy in mice. Cell. 2007; 130:427–439. [PubMed: 17693254]

30. Ray PS, Martin JL, Swanson EA, Otani H, Dillmann WH, Das DK. Transgene overexpression of alphaB crystallin confers simultaneous protection against cardiomyocyte apoptosis and necrosis during myocardial ischemia and reperfusion. FASEB J. 2001; 15:393–402. [PubMed: 11156955]
31. Suzuki A, Sugiyama Y, Hayashi Y, Nyu-i N, Yoshida M, Nonaka I, Ishiura S, Arahata K, Ohno S. MKBP, a novel member of the small heat shock protein family, binds and activates the myotonic dystrophy protein kinase. J Cell Biol. 1998; 140:1113–1124. [PubMed: 9490724]
32. Swamynathan SK, Piatigorsky J. Orientation-dependent influence of an intergenic enhancer on the promoter activity of the divergently transcribed mouse Shsp/alpha B-crystallin and Mkbp/HspB2 genes. J Biol Chem. 2002; 277:49700–49706. [PubMed: 12403771]
33. Taylor RP, Benjamin IJ. Small heat shock proteins: a new classification scheme in mammals. J Mol Cell Cardiol. 2005; 38:433–444. [PubMed: 15733903]
34. Veksler VI, Kuznetsov AV, Sharov VG, Kapelko VI, Saks VA. Mitochondrial respiratory parameters in cardiac tissue: a novel method of assessment by using saponin-skinned fibers. Biochim Biophys Acta. 1987; 892:191–196. [PubMed: 3593705]
35. Vicart P, Caron A, Guicheney P, Li Z, Prevost MC, Faure A, Chateau D, Chapon F, Tome F, Dupret JM, Paulin D, Fardeau M. A missense mutation in the alphaB-crystallin chaperone gene causes a desmin-related myopathy. Nat Genet. 1998; 20:92–95. [PubMed: 9731540]
36. Voos W. A new connection: chaperones meet a mitochondrial receptor. Mol Cell. 2003; 11:1–3. [PubMed: 12535512]
37. Voos W. Tom40: more than just a channel. Nat Struct Biol. 2003; 10:981–982. [PubMed: 14634628]
38. Yellon DM, Alkhulaifi AM, Pugsley WB. Preconditioning the human myocardium. Lancet. 1993; 342:276–277. [PubMed: 8101304]
39. Yellon DM, Hausenloy DJ. Realizing the clinical potential of ischemic preconditioning and postconditioning. Nat Clin Pract Cardiovasc Med. 2005; 2:568–575. [PubMed: 16258568]

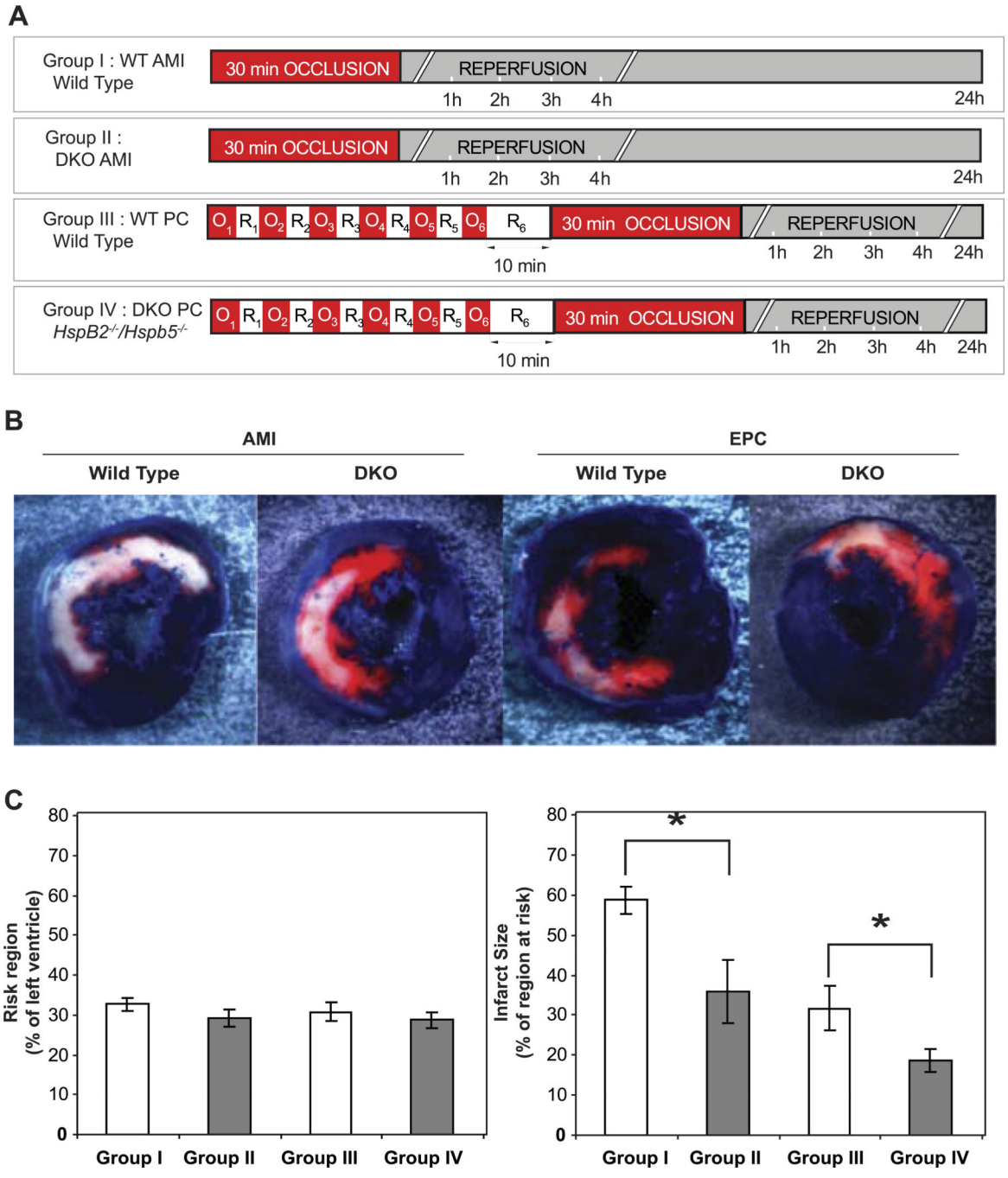

Fig. 1.

In situ analysis. *A*: indirect immunofluorescence analysis of heart sections stained with anti-CryAB detected by FITC-conjugated secondary antibodies shows CRYAB (green) in cardiomyocytes of wild-type (WT) but not in double knockout (DKO) hearts. No histomorphological abnormalities are seen for either WT or DKO hearts at 6 mo. *B*: protocols for acute myocardial infarction (AMI) without and with early preconditioning (EPC). *Group I* (WT; $n = 10$) and *group II* (DKO; $n = 11$) animals were subjected to 30 min occlusion followed by 24 h reperfusion. Preconditioning (PC) consisted of 6 cycles of 4 min of coronary occlusion (O) and 4 min of reperfusion (R), followed 10 min later, before prolonged 30 min occlusion and 24 h reperfusion. *Group III* (WT, early PC; $n = 11$) and

group IV (DKO, early PC; $n = 10$) Infarct size was determined with triphenyltetrazolium (TTC) staining and phthalo blue. TTC staining distinguishes the infracted (white) from viable (red) myocardial regions. Infarct size is qualitatively smaller in DKO and after early PC. *C*: myocardial infarct sizes in *groups I–IV* are quantitatively expressed as percentage of the risk region at risk. Data are means ± SE. $*P < 0.05$ vs. *group I*.

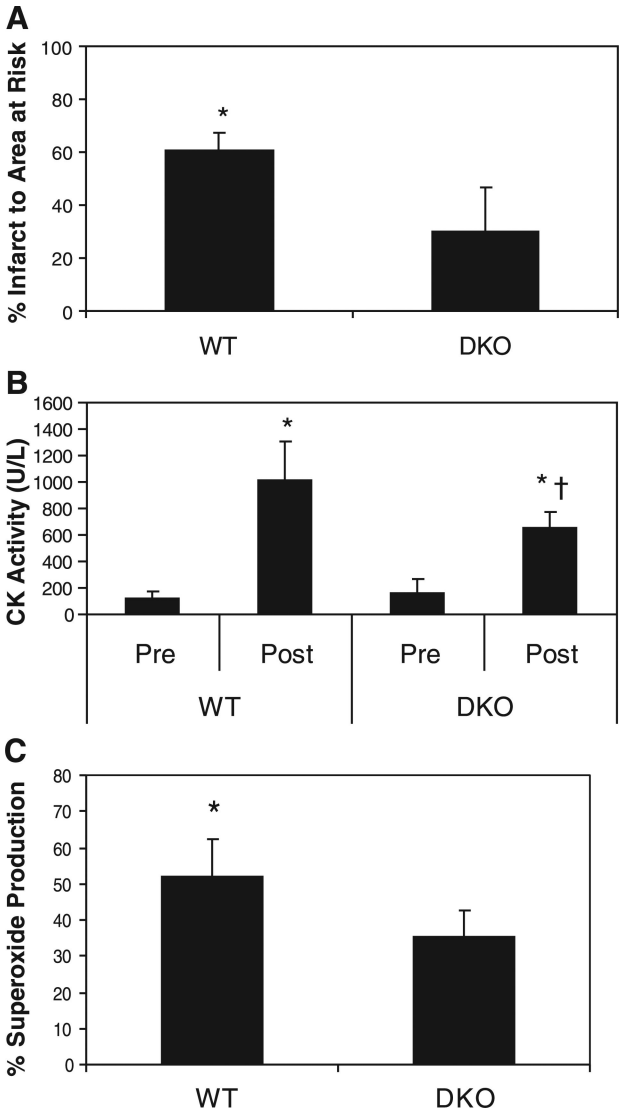

Fig. 2.

Ex vivo analysis. *A*: infarct size was similarly determined after reperfusion with TTC staining. The hearts of 4-mo-old animals were subjected to 30 min of global ischemia followed by 15 min (superoxide production) or 120 min (infarct size) of reperfusion. $*P < 0.05$; $n = 4$ WT and $n = 5$ DKO. *B*: creatine kinase (CK), a biomarker of myocardial injury, was assessed directly from the coronary effluent before (Pre) and following (Post) ischemia. $*P < 0.05$ vs. Pre value; $\dagger P < 0.05$ vs. WT Post; $n = 7$ WT and DKO. *C*: measurements of superoxide production were determined during and after reperfusion as described in MATERIALS AND METHODS. $*P < 0.05$; $n = 5$ WT and $n = 8$ DKO. Data are means ± SE.

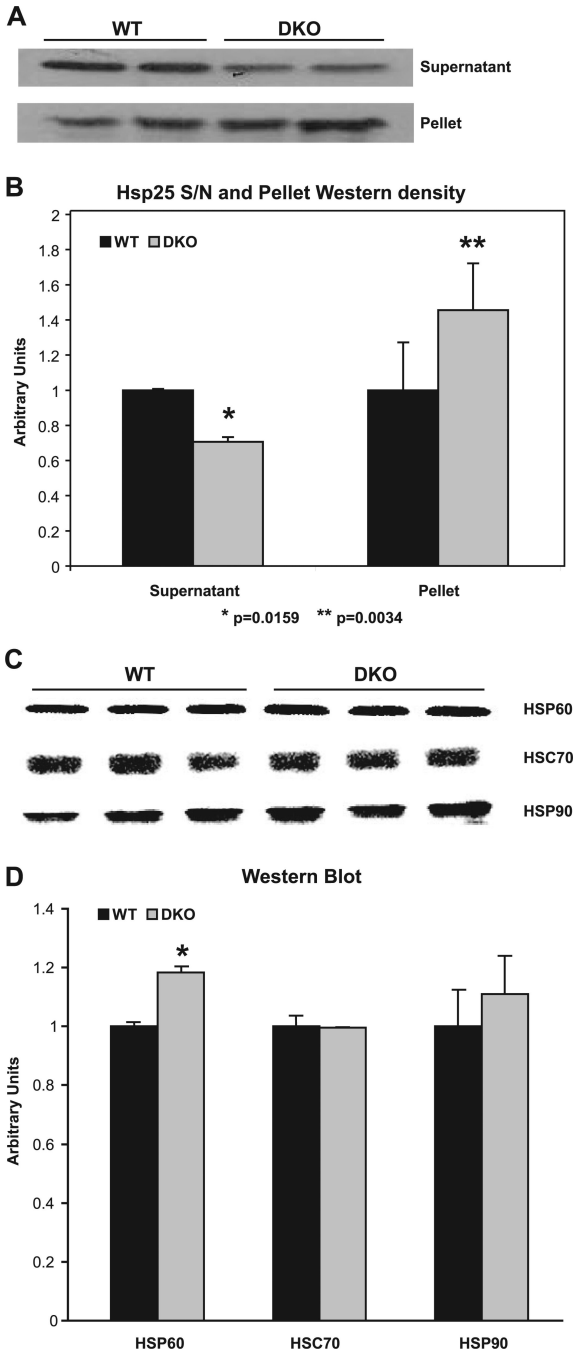

Fig. 3.

Western Blot. *A*: representative Western blot probed with anti-HSP25 antibody of either the soluble [supernatant (S/N)] or insoluble (pellet) fractions isolated from hearts of 6-mo-old WT and DKO animals. DKO is associated with modest downregulation of heat shock protein (HSP)25 in the cytosolic fraction and equivalent translocation into the cytoskeletal/nuclear fraction assessed by densitometry (*B*). Each lane represents an individual animal. Western blot analysis (*C*) and densitometry (*D*) were performed on cardiac homogenates of WT and CRYAB/HSPB2-deficient (DKO) for HSP60, HSP70, and HSP90. Each lane represents an individual animal in either the WT or DKO experimental groups ($n = 3$/group). $*P < 0.05$.

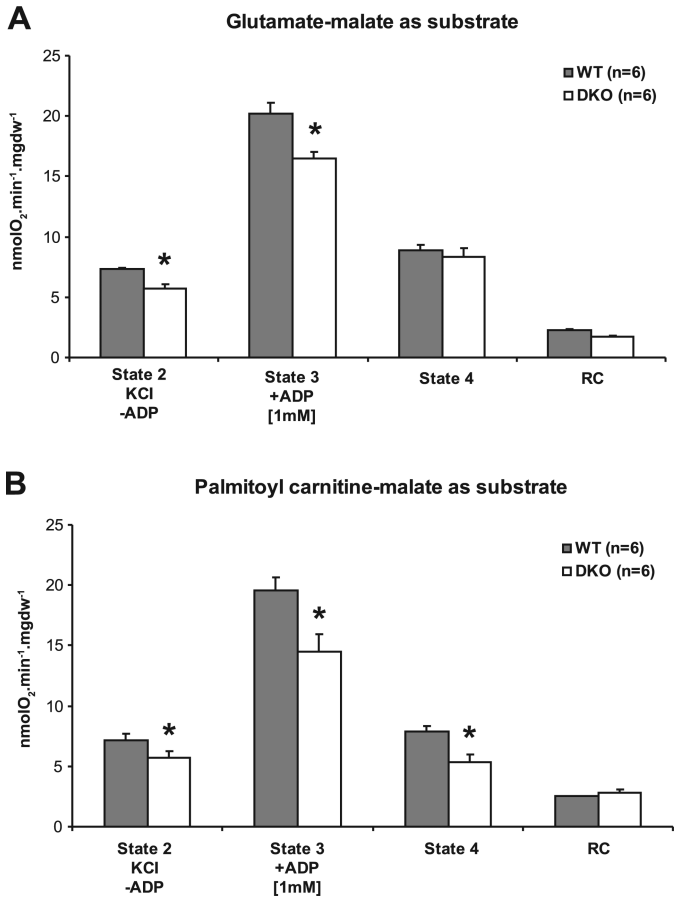

Fig. 4.

Respiration in cardiac fibers. Mitochondrial respiratory parameters were obtained from permeabilized fibers incubated with glutamate-malate (*A*) and palmitoyl carnitine-malate (*B*) as substrates. Gray bars, fibers obtained from the glucose-perfused WT hearts ($n = 6$); white bars, fibers from CRYAB/HSPB2-deficient (DKO) hearts ($n = 6$). Mitochondria was harvested from hearts of 6–8-wk-old animals. State 2, respiration in the absence of ADP; state 3, respiration ADP (1 mmol/l)-stimulated respiration; state 4, oligomycin (1 μg/ml)-inhibited respiration; RC, respiratory control ratio. Values are shown as means ± SE. $*P < 0.05$. State 3 respiratory was significantly lower with both substrates in DKO compared with WT. Mgdw, milligrams of dry weight.

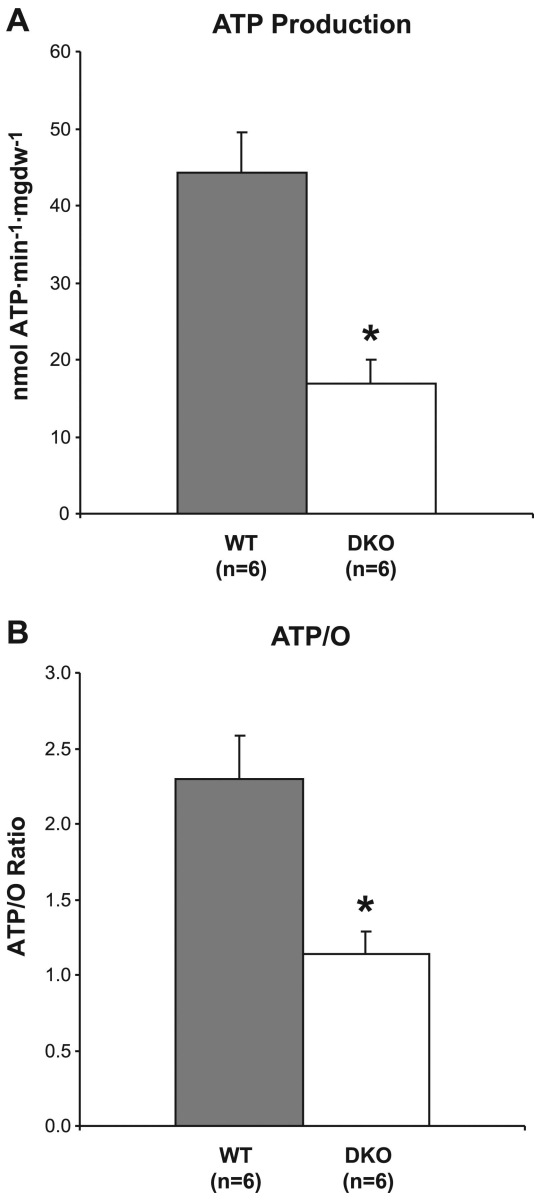

Fig. 5.

ATP in cardiac fibers. ATP rates and ATP-to-O ratios (ATP/O) obtained from permeabilized fibers, where O refers to oxygen consumption under state 3 conditions. ATP production was measured by a bioluminescence assay initiated by the addition of 1 mM ADP to the skinned fiber preparation. ATP synthesis rates were significantly lower in DKO fibers from hearts of 6–8-wk-old animals compared with WT. Values are shown as means ± SE.

Table 1

Size of LV, risk region, and infarct

	n	Male/Female	BW, g	Age, wk	LV, mg	RAR, mg	Infarct, mg	RAR, %LV	Infarct Size, %RAR
Group I	10	8/2	27.5±1.1	35.4±3.13	118±6	38± 2	23±2	32.7±1.7	58.8±3.4
Group II	11	5/6	26.0±1.2	33.4±11.3	117±9	34± 3	13±3 *	29.1±2.1	36.0±7.9 ‡
Group III	11	5/6	26.0±1.3	18.1±3.2	110±5	34±3	11±2	30.8±2.5	31.7±5.5
Group IV	10	6/4	27.4±1.1	21.7±8.4	131±8	37± 3	7±2 †	28.7±2.1	18.7±3.0 §

Values are means ± SE; *n*, number of animals. Statistical comparisons of infarct size were adjusted for sex and age using multivariable linear regression, with *P* values adjusted for 6 multiple comparisons using Finner's procedure (Ref. 6). BW, body weight; LV, left ventricle; RAR, region at risk. Infarct column:

Unadjusted $P < 0.05$ vs. *group 1*. The ages for groups subjected to either AMI (*groups I* and *II*) or early PC (*groups III* and *IV*) were similar.

* $P < 0.05$ vs. *group I.*

‡ $P < 0.001$ vs. *group I.* Infarct size column:

† $P < 0.05$ vs. *group I.*

§ $P < 0.001$ vs. *group I.* There was no significant group difference in sex ($P = 0.368$).